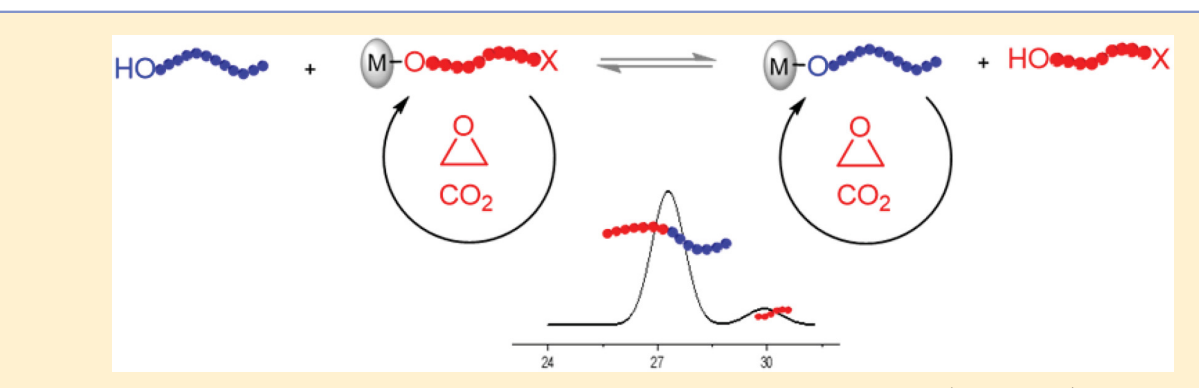
Synthesis of CO₂-Based Block Copolymers via Chain Transfer Polymerization Using Macroinitiators: Activity, Blocking Efficiency, and Nanostructure

Yao-Yao Zhang,[†] Guan-Wen Yang,[†] Yanyan Wang,[‡] Xin-Yu Lu,[†] Guang-Peng Wu,*,[†] Ze-Sheng Zhang,[†] Kai Wang,^{†,§} Ruo-Yu Zhang,[†] Paul F. Nealey,^{§,||©} Donald J. Darensbourg,*,^{‡,©} and Zhi-Kang Xu[†]

Materials Science Division, Argonne National Laboratory, 9700 S. Cass Avenue, Argonne, Illinois 60439, United States



ABSTRACT: Immortal copolymerization of epoxides/CO₂ using macro-chain-transfer agent (macro-CTA) is a useful method to prepare CO₂-based block copolymers for manufacturing high value-added materials. Despite a variety of CO₂-based block copolymers that have been reported using distinct macro-CTAs, issues including catalytic activity and blocking efficiency for the immortal polymerization remain superficially understood. Here, we systematically studied the reaction activity and blocking efficiency by using various macro-CTAs (including PPG, PEG, and PS) in the presence of two classical catalyst systems ((BDI)ZnOAc and SalenCoTFA/PPN-TFA). By analysis of the gel permeation chromatograms via mathematical deconvolution, it comes to a conclusion that the size, nature, and ratio of [macro-CTA]/[Cat.] strongly influence the catalytic activity of the reaction and blocking efficiency for the resultant block copolymers. Thin film self-assembly of PS/PPC block copolymers was investigated, and the results were analyzed by SEM to ascertain the impact of blocking efficiency on nanoassembly.

■ INTRODUCTION

The synthesis of polycarbonates via copolymerization of CO₂ and epoxides offers an opportunity to replace partially petroleum resources, as CO2 is an abundant and renewable C1 source.¹⁻⁴ Compared with the current polycarbonate production technology, this transformation circumvents the challenges involved with hypertoxic phosgene or phosgene derivatives.⁵ Concurrently with the development of catalyst systems, 6-14 CO₂-based polycarbonates with high thermoresistance, fascinating topologies, functional groups, and crystalline property have been well developed to improve material performance as well as product type. 15-24

Among various strategies to modify the thermal and mechanical properties of the CO2-based materials, the preparation of block copolymers (BCPs) by incorporating different macromolecular blocks is emerging as a useful

method.^{25–29} Up to now, two main strategies have been explored for synthesis of block copolymers incorporating CO₂/ epoxides and other monomers (Scheme 1). One approach involves the addition of a monomer that copolymerizes with epoxides at a much faster rate than CO₂. 30,31 In 2008, Coates and co-workers reported the first example of polyester-blockpolycarbonate polymers via terpolymerization of diglycolic anhydride (DGA), cyclohexene oxide (CHO), and CO₂. The relating mechanism studies indicated that the high reactivity of DGA completely suppressed the incorporation of CO₂ into the polymer chain; thus, CO₂/CHO alternating insertion could not occur until all the anhydride had reacted, giving the well-

Received: October 19, 2017 Revised: January 16, 2018 Published: February 1, 2018

[†]MOE Key Laboratory of Macromolecular Synthesis and Functionalization, and Key Laboratory of Adsorption and Separation Materials & Technologies of Zhejiang Province, Department of Polymer Science & Engineering, Zhejiang University, Hangzhou 310027, China

[‡]Department of Chemistry, Texas A&M University 3255 TAMU, College Station, Texas 77843, United States

[§]Institute for Molecular Engineering, University of Chicago, Chicago, Illinois 60637, United States

Scheme 1. Methods for Synthesis CO₂-Based Block Copolymers: (a) Terpolymerization of Anhydrides, CO₂, and Epoxides; (b) Using Macro-Chain-Transfer Agent in the Copolymerization of Epoxides and CO₂

defined polyester/polycarbonate block copolymers. Subsequently, many polyester/polycarbonate block and/or gradient copolymers were well developed by terpolymerizations of different epoxides and various anhydrides with $\mathrm{CO_2}$. By replacing cyclic anhydride with β -butyrolactone (BBL), Rieger and co-workers prepared poly(hydroxybutyrate)/poly(cyclohexene carbonate) block copolymers in a one-pot copolymerization of $\mathrm{CO_2}$, BBL, and CHO by switch on/off $\mathrm{CO_2}$ during the polymerization.

An alternative approach for the preparation of CO2-based block copolymers involves a polymer with a terminal initiating site that can be used as a macro-chain-transfer agent (macro-CTA) to incorporate epoxides/CO₂. ^{38,39} Under these circumstances, as indicated in Scheme 1b, chain propagation is first initiated by the ring-opening of the coordinated epoxide by the nucleophilic anion (X⁻) to afford a metal-alkoxide intermediate. This active propagating chain is protonated by the macro-CTA, releasing a dormant PC-OH chain with endcapped X group and a M-CTA intermediate. The released M-CTA intermediate then serves as an active center to initiate the alternating incorporation of epoxide and CO2, giving the predesigned block copolymers. In contrast with a classical living polymerization where each initiating group of catalyst affords one polymer chain, chain transfer activity to the CTA allows the growth of several polymer chains on one catalyst molecule. This method is also referred to as immortal polymerization. ^{40,41} On the basis of this method, Lee reported the preparation of diand triblock copolymers by introducing polymers during the copolymerization of CO₂/epoxides. 42 Our group and Williams and co-workers have reported the preparation of polycarbonate/polylactide di- and triblock copolymers in a two-step process, respectively. 43-46 The first step involves the synthesis of a polycarbonate with end-capped hydroxyl groups, which can be used as macro-CTA subsequently to initiate the ringopening polymerization of lactide. In recent studies, poly-(dimethylsiloxane), poly(ethylene oxide), and polyolefin macro-CTAs have been performed to synthesize new CO₂-based block copolymers. 47–49 Based on this methodology, the thermoresistance, brittleness/softness, and hydrophilicity performances of CO₂-based polymers are well modified by incorporating distinct blocks.

In addition to the improvement in physical and mechanical properties, another driving force for synthesis of CO₂-based

block copolymers is to manufacture high value-added materials, particularly, motivated by their attractive phase separation behavior in the formation of nanomaterials. For example, we have reported the preparation of CO₂-based amphiphilic block copolymers, 44,50 which can self-assemble into micelles adopting diverse morphologies and dimensions in water, thereby exhibiting attractive properties for biomedical applications. Wiesner and Coates research groups coreported the synthesis and self-assembly studies of polyisoprene-block-polystyreneblock-poly(propylene carbonate) (PI-b-PS-b-PPC), ⁵¹ where PI and PPC blocks could be degraded and backfilled independently, leaving periodically ordered complex nanoreactors. More recently, we have found that polystyrene-block-poly(propylene carbonate) (PS-b-PPC) is well qualified to fill key positions on the directed self-assembly strategy for the next-generation lithography because of its sub-10 nm domains, nearly equal surface energies between blocks, and the ability for pattern transfer.52

A variety of CO₂-based block copolymers have been reported using distinct macro-CTAs; 42-49 however, issues for the immortal polymerization involved from the macro-CTAs remain superficially understood. 53,54 These issues include (1) whether all the added macro-CTAs can participate in the polymerization, especially, once the added macro-CTA is incompatible with the polycarbonate block; (2) how the molecular weight and/or the amount of the macro-CTA influence the catalytic activity and the chain extension efficiency; and (3) the amount of the CO₂-PC impurities (PC-X) generated in the immortal polymerization needs evaluation (Scheme 1b), since the properties of the assembled nanostructure are predominantly dependent on the purity of the BCPs product. For example, Stoykovich et al. found that the accurate loading of homopolymer into block copolymers could facilitate the periodic assemble arrays for nanoscale manufacturing.⁵⁵ On the basis of these questions, we herein communicate our initial studies for preparation of well-defined CO₂-based block copolymers by using different macro-CTAs with an aim to evaluate their influence on activity and blocking efficiency. By analysis of the gel permeation chromatograms (GPC) via mathematical deconvolution, the reaction activity and blocking efficiency for the resulting immortal polymerizations are evaluated. From these studies, it is believed that the nature of the chain transfer agents and the ratios of macro-CTA to catalyst as well as the molecular weight of the macro-CTA significantly affect the activity and the blocking efficiency during the reaction. Furthermore, we intend to describe the influence of the blocking efficiency on their thin film self-assembly behavior of the thereby obtained block copolymers.

EXPERIMENTAL SECTION

General Information. All manipulations involving air- and/or water-sensitive compounds were carried out in a glovebox under a nitrogen atmosphere. Propylene epoxide and cyclohexene oxide (Sigma-Aldrich) were stirred over CaH₂ distilled and stored in an N₂-filled glovebox. The CO₂ (research grade 99.999%) was further purified by passing through two steel columns packed with 4 Å molecular sieves that had been dried under vacuum at ≥200 °C. The 50 mL high-pressure stainless steel reactor (Anhui Kemi Machinery Technology Co., Ltd.) was previous dried at 150 °C for 24 h prior to use in the copolymerization. Catalysts 1 and 2 were prepared following the procedures in refs 56 and 57. Macro-CTA including α , ω -dihydroxy end-capped poly(ethylene glycol) (PEG), poly(propylene glycol) (PPG), polystyrene (PS-OH), and poly(N-isopropylacrylamide)

(PNIPAM) polymers, with different molecular weights, were purchased from Polymer Source Inc.

Analysis. ¹H NMR (400 MHz) and ¹³C NMR (100 MHz) were carried out in chloroform-d on a Bruker DPX 400 MHz spectrometer. DSC measurements were performed on a NETZSCH DSC 214 Polyma instrument (NETZSCH, Germany) equipped with an IC70 intracooler and the temperatures range from -65 to 160 °C at heating/cooling rates of 10 K/min under nitrogen. Temperature and heat flow were calibrated by an indium standard. The glass transition temperature (T_g) was taken as the midpoint of the inflection tangent, upon the third heating scan. GPC was conducted on a system equipped with a Waters Chromatography, Inc., model 1515 isocratic pump, a model 2414 differential refractometer, and a three-column set of Polymer Laboratories, Inc. Styragel columns (PLgel 5 μmMixed C, 500 and 104 Å, 300 \times 7.5 mm columns). The system was equilibrated at 35 °C in THF which served as the polymer solvent with 1.00 mL/ min flow rate. Polymer solutions were prepared at a known concentration (ca. 5 mg/mL), and an injection volume of 50 μL was used. The dn/dc values of the analyzed polymers were determined using refractive index detector data. A Hitachi CG5000 scanning electronic microscope (SEM) was used to image the assembled block copolymer films after reactive ion etching.

Representative Procedure for Synthesis of CO₂-Based BCP in the Presence of Macro-CTA. In a drybox, catalyst and macro-CTA were dissolved in epoxide under N2. The solution was charged into a predried 50 mL autoclave equipped with an in situ infrared Re \actIR ic15 reaction analysis system (purchased from Mettler Toledo). The system was pressurized to the appropriate pressure with CO₂, and the infrared spectrometer was set to collect one spectrum every 15 s over the corresponding reaction time. Profiles of the absorbance at 1750 cm⁻¹ for polycarbonate with time were recorded after baseline correction. After the allotted reaction time, the CO₂ pressure was slowly released, and a small amount of the resultant polymerization mixture was removed from the autoclave for ¹H NMR analysis to determine the conversion of epoxide and GPC analysis to determine the blocking efficiency. The crude polymer was dissolved in a small amount of CH₂Cl₂, and a large amount of cold methanol or pentane (depending on the macro-CTA used) was added for polymer precipitation. To get purified BCP, the dissolving/precipitation process and/or chromatography purification were repeated multiple times until the residual PC and CTA homopolymers were completely removed, and then the white CO2-based BCP was obtained by vacuum-drying. The representative ¹H NMR, ¹³C NMR shifts, and DSC measurements of each block polymer are shown as follows.

Poly(cyclohexene carbonate)-block-poly(ethylene glycol)-block-poly(cyclohexene carbonate) (PCHC-b-PEG-b-PCHC). $T_{\rm g}=77.6^{\circ}$ C. ¹H NMR (chloroform-d, 400 MHz, ppm): δ 4.65 (br, -OCOO-CH-CH $_{2}$ CH $_{2}$), 3.65 (s, -O-CH $_{2}$ CH $_{2}$), 2.11 (br, -OCOO-CH-CH $_{2}$ CH $_{2}$), 1.70 (br, -OCOO-CH-CH $_{2}$ CH $_{2}$), 1.57–1.34 (br, m, -OCOO-CH-CH $_{2}$ CH $_{2}$). ¹³C NMR (chloroform-d, 100 MHz, ppm): δ 153.8, 76.5, 70.5, 29.4, 22.8.

Poly(cyclohexene carbonate)-block-poly(propylene glycol)-block-poly(cyclohexene carbonate) (PCHC-b-PPG-b-PCHC). $T_{\rm g}=95.6$ °C. ¹H NMR (chloroform-d, 400 MHz, ppm): δ 4.65 (br, -OCOO-CH-CH $_2$ -CH $_2$ -), 3.56 (br, m, -O-CH $_2$ -CH(CH $_3$)-), 3.41 (br, m, -O-CH $_2$ -CH(CH $_3$)-), 2.11 (br, -OCOO-CH-CH $_2$ -CH $_2$ -), 1.70 (br, -OCOO-CH-CH $_2$ -CH $_2$ -), 1.57-1.34 (br, m, -OCOO-CH-CH $_2$ -CH $_2$ -), 1.13 (br, m, -O-CH $_2$ -CH(CH $_3$)-). ¹³C NMR (chloroform-d, 100 MHz, ppm): δ 153.8, 76.5, 75.3, 73.3, 29.4, 22.8, 17.3.

Poly(cyclohexene carbonate)-block-polystyrene-block-poly(cyclohexene carbonate) (PCHC-b-PS-b-PCHC). $T_{\rm g}=105.0$ °C. $^{1}{\rm H}$ NMR (chloroform-d, 400 MHz, ppm): δ 7.09–6.52 (br, m, C₆H₅–CH–CH₂–), 4.65 (br, —OCOO–CH–CH₂–CH₂–), 2.11 (br, —OCOO–CH–CH₂–CH₂–), 1.84 (br, C₆H₅–CH–CH₂–), 1.70 (br, —OCOO–CH–CH₂–CH₂–), 1.57–1.34 (br, m, —OCOO–CH–CH₂–CH₂–), 1.43 (br, C₆H₅–CH–CH₂–). $^{13}{\rm C}$ NMR (chloroform-d, 100 MHz, ppm): δ 153.8, 145.4, 128.0, 125.7, 76.5, 43.8, 40.3, 29.5, 22.9.

Poly(propylene carbonate)-block-poly(ethylene glycol)-block-poly(propylene carbonate) (PPC-b-PEG-b-PPC). $T_{\rm g}=15.2\,^{\circ}{\rm C.}^{1}{\rm H}$ NMR (chloroform-d, 400 MHz, ppm): δ 5.01 (br, $-{\rm OCOO-CH_2-CH(CH_3)-}$), 4.20 (br, m, $-{\rm OCOO-CH_2-CH(CH_3)-}$), 3.65 (s, $-{\rm O-CH_2-}$), 1.33 (d, J=6.4 Hz, $-{\rm OCOO-CH_2-CH(CH_3)-}$). $^{13}{\rm C}$ NMR (chloroform-d, 100 MHz, ppm): δ 154.2, 72.3, 70.4, 68.9, 16.1.

Poly(propylene carbonate)-*block*-poly(propylene glycol)-*block*-poly(propylene carbonate) (PPC-*b*-PPG-*b*-PPC). $T_{\rm g}=25.0\,^{\circ}{\rm C.}^{1}{\rm H}$ NMR (chloroform-*d*, 400 MHz, ppm): δ 5.01 (br, $-{\rm OCOO-CH_2-CH(CH_3)-}$), 3.56 (br, m, $-{\rm O-CH_2-CH(CH_3)-}$), 3.41 (br, m, $-{\rm O-CH_2-CH(CH_3)-}$), 1.33 (d, J=6.4 Hz, $-{\rm OCOO-CH_2-CH(CH_3)-}$), 1.13 (br, m, $-{\rm O-CH_2-CH(CH_3)-}$), 1.3° C NMR (chloroform-*d*, 100 MHz, ppm): δ 154.2, 75.3, 73.3, 72.3, 68.9, 17.3, 16.1.

Poly(propylene carbonate)-block-polystyrene-block-poly(propylene carbonate) (PPC-b-PS-b-PPC). $T_g=38.9,\ 92.3\ ^{\circ}$ C. 1 H NMR (chloroform-d, 400 MHz, ppm): δ 7.09–6.52 (br, m, C_6H_5 –CH–CH₂–), 5.01 (br, –OCOO–CH₂–CH(CH₃)–), 4.20 (br, m, –OCOO–CH₂–CH(CH₃)–), 1.84 (br, C_6H_5 –CH–CH₂–), 1.43 (br, C_6H_5 –CH–CH₂–), 1.33 (d, J=6.4 Hz, –OCOO–CH₂–CH(CH₃)–). 13 C NMR (chloroform-d, 100 MHz, ppm): δ 154.2, 145.6, 128.2, 125.6, 75.3, 68.9, 43.8, 40.4, 16.1.

Self-Assembly Studies of the PPC-b-PS-b-PPC Block Copolymer Thin Films. Hydroxyl-terminated random copolymers of styrene and methyl methacrylate (PS-r-PMMA-OH), with styrene mole fractions ($f_{\rm st}$) of 0.12, were synthesized as before. The PS-r-PMMA-OH was spin-coated from a 0.5 wt % toluene solution onto the silicon wafer. The substrate was then annealed at 190 °C for 4 h to graft, via a condensation reaction, resulting in a 5 nm thick layer of PS-r-PMMA. Excess unreacted PS-r-PMMA-OH was washed away with toluene by sonication after the reaction. A PPC-b-PS-b-PPC film with ~20 nm thickness was spin-coated on the PS-r-PMMA-OH modified silicon wafer from a 0.5 wt % solution in toluene and annealed for 1 h at 150 °C in a nitrogen environment. Subsequently, the sample was imaged by SEM after reactive ion etching.

RESULTS AND DISCUSSION

Quantification of Blocking Efficiency. The quantity of block copolymers relative to homopolymer impurities is often referred to as blocking efficiency (E). 58,59 The GPC coupled with the mathematical deconvolution of the GPC traces was used to estimate the blocking efficiency for each polymerization, as the GPC curve of each polymer is ideal to the symmertrical Gaussian curves. 60 This method is based on the fact that the intensity of GPC signal (RI) is proportional to the dn/dc value of the polymer solute. Values of dn/dc for poly(propylene carbonate) (PPC), poly(cyclohexene carbonate) (PCHC), and poly(propylene glycol) (PPG) were determined as 0.0565, 0.0891, and 0.0550 mL/g, respectively, using response vs concentration plots from the differential refractometer. The dn/dc values for polystyrene (0.1860 mL/g) and poly(ethylene glycol) (PEG) (0.0740 mL/g) were taken from the literature.⁵⁸ As discussed in the preceding section, preparation of BCPs by using macro-CTA in Scheme 1, three kinds of polymers, i.e., block copolymer, homo-polycarbonate initiated by X, and unreacted macro-CTA, may appear on their GPC traces. Thus, the blocking efficiency (E_{cal}) was calculated with respect to their dn/dc by eq 1:

$$E_{\text{cal}} = \frac{A_{\text{BCP}} / \left(\frac{dn}{dc}\right)_{\text{BCP}}}{A_{\text{BCP}} / \left(\frac{dn}{dc}\right)_{\text{BCP}} + A_{\text{CTA}} / \left(\frac{dn}{dc}\right)_{\text{CTA}} + A_{\text{PC}} / \left(\frac{dn}{dc}\right)_{\text{PC}}}$$
(1)

where the areas of the three GPC peaks ($A_{\rm BCP}$, $A_{\rm PC}$, and $A_{\rm CTA}$) are obtained via the Origin Peak Analyzer. The dn/dc values of

Figure 1. Utilized catalyst systems and macro-CTAs.

Table 1. Effects on Macro-CTAs during CO₂/CHO Copolymerization Catalyzed by 1^a

entry	СТА	$M_{ m n,CTA}^{0$	$PDI_{CTA}^{b} (M_{\rm w}/M_{\rm n})$	CTA/Cat. (mole ratio)	t (h)	conv ^c (%)	TOF^{c} (h^{-1})	$M_{ m n,BCP}^{c}$ (kg/mol)	$PDI_{BCP}^{d} (M_{\scriptscriptstyle W}/M_{\scriptscriptstyle n})$	$\frac{E_{\mathrm{theo}}^{e}}{(\%)}$	$\frac{E_{\mathrm{cal}}^{f}}{(\%)}$
1	none				4	64.1	160	_g	_g	g	_g
2	PPG	2.0	1.01	1/1	4	55.7	149	41.3	1.03	67	50
3	PPG	2.0	1.01	5/1	4	33.8	85	9.8	1.05	91	81
4	PPG	4.0	1.03	1/1	4	51.8	130	37.6	1.04	67	46
5	PPG	4.0	1.03	5/1	4	27.0	67	9.8	1.04	91	76
6	PEG	2.0	1.02	1/1	4	46.5	116	29.6	1.02	67	42
7	PEG	2.0	1.02	5/1	4	32.2	81	8.7	1.06	91	74
8	PEG	4.0	1.03	1/1	4	35.0	88	21.8	1.07	67	40
9	PEG	4.0	1.03	5/1	4	18.0	45	7.4	1.02	91	67
10	PS-OH	6.0	1.02	1/1	4	47.4	119	39.4	1.03	67	50
11	PS-OH	12.5	1.04	1/1	4	21.3	53	25.1	1.04	67	42
12	PNIPAM	6.0	1.06	1/1	12	0	0	_g	_g	67	_g

"Experimental procedure: complex 1 (0.05 mmol) and CTA with different amounts were dissolved in CHO (50 mmol) in glovebox, and then the mixture was carefully injected into a homemade 50 mL predried autoclave, which was equipped with an *in situ* infrared ReactIR ic15 reaction analysis system with a SiComp ATR crystal. The autoclave was heated up to 50 °C and then was pressurized to 3.0 MPa CO₂. After 4 h, the CO₂ pressure was slowly released and a small amount of the resultant polymerization mixture was removed from the autoclave for ¹H NMR analysis to determine the conversion of CHO and GPC analysis. ^bPurchased from Polymer Source Inc. and confirmed by GPC. ^cDetermined by ¹H NMR spectroscopy. ^dDetermined by GPC against polystyrene standard using THF as eluent. ^cObtained using eq 3. ^fObtained following eqs 1 and 2. ^gNot applicable.

pure block copolymers could be calculated based on the weight fraction of two blocks $(W_{\rm CTA}, W_{\rm PC})$ shown in eq 2:

$$\left(\frac{\mathrm{d}n}{\mathrm{d}c}\right)_{\mathrm{BCP}} = W_{\mathrm{CTA}} \left(\frac{\mathrm{d}n}{\mathrm{d}c}\right)_{\mathrm{CTA}} + W_{\mathrm{PC}} \left(\frac{\mathrm{d}n}{\mathrm{d}c}\right)_{\mathrm{PC}} \tag{2}$$

To compare the chain transfer ability of CTAs under certain conditions, theoretical chain transfer efficiency ($E_{\rm theo}$) is defined by eq 3:

$$E_{\text{theo}} = \frac{N_{\text{OH}}}{N_{\text{OH}} + N_{\text{X}}} \tag{3}$$

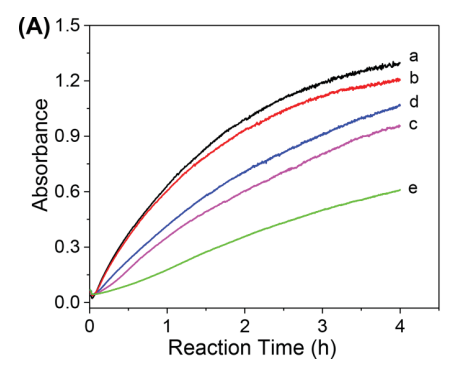
where $N_{\rm OH}$ corresponds to the mole number of hydroxyl groups of macro-CTA, and $N_{\rm X}$ corresponds to the mole number of nucleophilic anion (X⁻) on the catalyst. It should be noted here that this equation is based on the assumption that all the active species exhibit the same chain transfer capacity.

Catalyst Systems and Macro-Chain-Transfer Agents. Two state-of-the-art catalyst systems, (BDI)ZnOAc (BDI = β -diiminate) 1 and SalenCoTFA/PPN-TFA (TFA = trifluor-oacetate, 1/1 molar ratio) 2, were selected for this study, since their detailed mechanism studies and the controlled polymerization behavior for epoxide/CO₂ coupling reaction are well established (Figure 1). S6,61-68 Several α , ω -dihydroxy end-capped polymers, i.e., PEG, PPG, PS-OH, and PNIPAM, were used with varied molecular weight and additional amount

to gain access to their influence on the reaction activity and blocking efficiency, and each macro-CTA displays unimodality with quite narrow polydispersity (PDI < 1.05).

Influence of Macro-CTAs on Catalytic Activity during CHO/CO₂ Copolymerization Using (BDI)ZnOAc Complex. Initially, we examined the copolymerization of CHO and CO₂ employing the (BDI)ZnOAc system (1). Before evaluation of the immortal polymerization with different macro-CTAs, a control experiment that copolymerization of CHO and CO₂ in the absence of macro-CTAs was conducted (Table 1). The optimal loading for the CHO/CO₂ copolymerization with 1 was at [CHO]:[Zn] ratio of 1000:1 with 3.0 MPa CO_2 pressure. Under these conditions, PCHC is generated in 64.1% yield after 4 h, corresponding to catalytic activity of 160 turnovers per hour (TOF, entry 1, Table1) with only trace polyether linkages on PCHC backbone. A predictable molecular weight with narrow polydispersity (M_n) = 67K, PDI = 1.03) demonstrates the controlled polymerization behavior (entry 1 in Table 1).69

To systematically study the influence of the macro-CTAs on CHO/CO₂ catalytic activity under 1, four kinds of macro-CTAs (including PEG, PPG, PS-OH, and PNIPAM) with different molecular weights and varied ratios of [macro-CTA]/[Zn] were investigated (Table 1). All polymerizations were monitored by *in situ* IR, and the reaction conditions were fixed at [CHO]:[1] = 1000:1, 3.0 MPa of CO₂, and 4 h. The bimodal



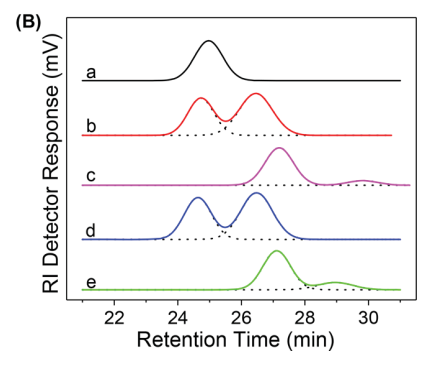


Figure 2. (A) Reaction profile of the IR spectra at 1750 cm⁻¹ collected during the immortal CHO/CO₂ copolymerization in the presence of 1 with PPGs, and (B) the relating GPC traces of the polymerization mixture after 4 h. (a) Without CTA; (b) $[PPG_{2K}]/[1] = 1/1$; (c) $[PPG_{2K}]/[1] = 5/1$; (d) $[PPG_{4K}]/[1] = 1/1$; (e) $[PPG_{4K}]/[1] = 5/1$ (mole ratio). The 1750 cm⁻¹ is the absorbance of the carbonyl group in PCHC.

weight distribution and the disappearance of macro-CTAs signal on the GPC traces of all resultant polymers indicate successful chain extension from the ends of macro-CTAs (Figure 2B). The elution time of the high molecular weight shoulder present in the chromatogram was assigned to the block copolymers due to the increasing hydrodynamic volume, while the elution time of the low molecular weight shoulder was assigned to PCHC homopolymers that initiated from X (acetate) on catalyst (Scheme 1b).

All reactions display much lower or even no reactivity (Table 1) compared to the copolymerization of CHO/CO₂ without the addition of macro-CTA. For instance, with 1 equiv of PPG_{2K} ($M_n = 2.0 \text{ kg/mol}$), the TOF of 1 decreased to 149 h⁻¹, while the catalytic activity for CHO further decreased to 85 h⁻¹ after 5 equiv of PPG_{2K} was intentionally added (entries 2 and 3, Table 1). Upon the molecular weight of PPG increasing to 4.0 kg/mol, further compromised catalytic activities for CHO turnovers per hour 130 and 67 h⁻¹, were clearly observed upon addition of 1 and 5 equiv of PEG4K into the reaction, respectively. A similar trend was also observed when PEG and hydroxyl end-capped PS were used as the macro-CTAs during the CHO/CO₂ immortal copolymerization (entries 6–11, Table 1), where negative effects on the reaction were clearly observed after increasing the molecular weight of macro-CTA and ratios of the [macro-CTA]/[1]. At $[PEG_{2K}]/[1] = 1/1$ and 5/1, immortal copolymerization of CHO/CO₂ reached 46.5% and 32.2% conversion in 4 h, while the copolymerization with PPG_{4K} achieved only 35.0% and 18.0%, respectively, under the same conditions (entries 6-9, Table 1). The TOF of 1 sharply decreased from 119 h⁻¹ with PS-OH_{6K} to 53 h⁻¹ when the molecular weight of PS-OH doubled (entries 10 and 11, Table 1). These results clearly indicate that the reactivity decreased with an increase of molecular weight and the added amount of macro-CTAs in CHO/CO₂ immortal copolymerizations.

The dramatic influence on the activity caused by different macro-CTAs was observed in the immortal copolymerization of CHO/CO₂ under 1. For instance, PPG and PEG share similar chemical structure with only one carbon difference; however, great differences were detected when they worked as macro-CTAs. After addition of 1 equiv of PPG_{2k}, the catalytic activity toward CHO was 149 h⁻¹, while the TOF of 1 decreased to $116 \, h^{-1}$ when PEG with the same molecular weight and ratio to 1 was applied. This trend was much clear when PPG_{4K} and PEG_{4K} were utilized as macro-CTAs during the immortal copolymerization (entries 4,5, 8, and 9, Table 1). On the basis of these results, it is clear that the nature, the molecular weight,

and the amounts of macro-CTAs used in the reaction have a tremendous impact on the reactivity during the immortal CHO/CO₂ copolymerization. A possible interpretation for this reaction phenomenon is discussed in the ensuing paragraph.

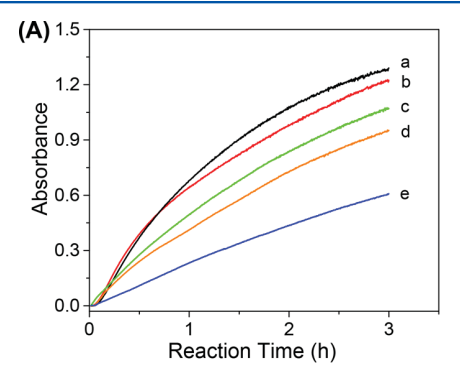
Influence of Macro-CTAs on Blocking Efficiency during CHO/CO₂ Copolymerization Using (BDI)ZnOAc Complex. Following the method used by Matyjaszewski et al., 59 the mathematical deconvolution of the GPC traces were used to estimate the blocking efficiency for each polymerization. As shown in Figure 2B, the final bimodal GPC curves were dealt with the mathematical deconvolution to give two unimodal components (dashed line); thus, the areas of the two peaks, A_{BCP} and A_{PCHC} , were obtained via the Origin Peak Analyzer. To evaluate the blocking efficiency, the resultant polymers obtained in each reaction were purified by repeated dissolving/precipitating process and chromatography until the residual PCHC homopolymers were completely removed. After ¹H NMR characterization, the polymer degree of the PCHC blocks of BCPs could be estimated by calculating the integral intensity of the methine (4.65 ppm) of the repeating PCHC unit to the characteristic peak of PEG (CH₂ at 3.65 ppm), PPG $(CH_3 \text{ at } 1.13 \text{ ppm}), \text{ and PS } (C_6H_5, 7.09-6.52 \text{ ppm}),$ separately. Based on the ¹H NMR calculation and GPC measurements, the composition, molecular weight, and dispersity for each block copolymers are provided in Table 1. Consequently, the values of dn/dc for the relating block copolymers could be calculated according to eq 2, and the blocking efficiency for each polymerization was obtained by using eq 1, and the results are provided in Table 1.

As shown in Table 1, the blocking efficiency was generally affected by the nature, molecular weight of macro-CTA, and the ratio of [macro-CTA]/[1]. For example, using 1 equiv of PPG_{2k} as macro-CTA yields PPG/PCHC block copolymers with 50% blocking efficiency. Increasing the molecular weight to 4.0 kg/mol, the blocking efficiency decreased to 46%, which is much lower than the theoretical value (67%). When the amounts of PPG_{2k} and PPG_{4k} were increased to 5 equiv, 81%and 76% blocking efficiency were observed, respectively (entries 2-5, Table 1). Substitution of PEG for PPG decreased the blocking efficiency of the resultant block copolymers. For example, when 1 and 5 equiv of amount of PEG_{2K} were applied, the blocking efficiency decreased to 42% and 74%, respectively (entries 6–9, Table 1). An increase of the molecular weight of PS resulted in a notable decrease in blocking efficiency of the resultant PS/PCHC block copolymers, under the same conditions (entries 10 and 11, Table 1). These experiments

Mad	cromolec	cul	les	Article
-----	----------	-----	-----	---------

entry	СТА	$M_{ m n,CTA}^{b}$ (kg/mol)	${ m PDI}_{ m CTA}^{b} \ (M_{ m w}/M_{ m n})$	CTA/Cat. (mole ratio)	t (h)	TOF^c (h^{-1})	$M_{ m n,BCP}^{c}$ (kg/mol)	$PDI_{BCP}^{d} (M_{ m w}/M_{ m n})$	$\frac{E_{\mathrm{theo}}^{e}}{(\%)}$	E_{cal}^f (%)
1	PEG	4.0	1.03	1/1	3	386	48.2	1.06	50	38
2	PEG	4.0	1.03	5/1	3	362	17.8	1.05	83	60
3	PEG	4.0	1.03	10/1	3	312	10.5	1.10	91	78
4	PEG	8.0	1.04	1/1	3	290	37.2	1.07	50	33
5	PEG	8.0	1.04	5/1	3	206	14.5	1.06	83	50
6	PPG	4.0	1.03	1/1	3	452	66.2	1.05	50	45
7	PPG	4.0	1.03	10/1	3	402	14.5	1.08	91	86
8	PPG	7.8	1.04	10/1	3	385	17.4	1.07	91	82
9	PS-OH	6.0	1.02	1/1	3	367	47.5	1.06	50	37
10	PS-OH	6.0	1.02	5/1	3	324	19.5	1.03	83	68
11	PS-OH	12.5	1.04	5/1	4	283	27.5	1.05	83	65
12	PS-OH	12.5	1.04	10/1	8	252	28.1	1.08	91	76

"Experimental procedure: complex 2 (0.05 mmol) and CTA with different amounts were dissolved in PO (150 mmol) in glovebox, and then the mixture was carefully injected into a homemade 50 mL predried autoclave, which was equipped with an *in situ* infrared ReactIR ic15 reaction analysis system with a SiComp ATR crystal. The autoclave was pressurized to 2.0 MPa of CO₂. After appropriate time, the CO₂ pressure was slowly released, and a small amount of the resultant polymerization mixture was removed from the autoclave for ¹H NMR analysis to determine the conversion of PO and GPC analysis. ^bObtained from Polymer Source Inc. and confirmed by GPC. ^cMeasured by ¹H NMR. ^dDetermined by GPC against polystyrene standard. ^eObtained using eq 3. ^fObtained using eqs 1 and 2.



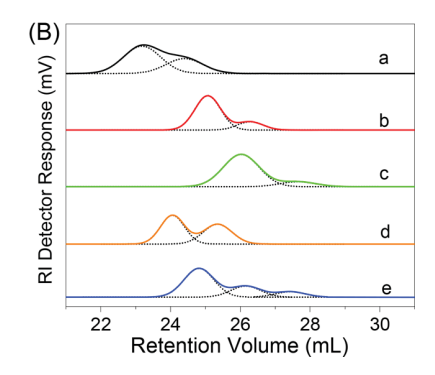


Figure 3. (A) Reaction profile of the IR spectra at 1750 cm⁻¹ collected every 15 s in the presence of 2 in PO with PEGs and (B) the relating GPC traces of the polymerization mixture after 3 h. (a) $[PEG_{4K}]/[2] = 1/1$; (b) $[PEG_{4K}]/[2] = 5/1$; (c) $[PEG_{4K}]/[2] = 10/1$; (d) $[PEG_{8K}]/[2] = 1/1$; (e) $[PEG_{8K}]/[2] = 5/1$ (mole ratio). The 1750 cm⁻¹ is the absorbance of the carbonyl group in PPC. Reaction conditions: [PO]/[SalenCoTFA]/[PPN-TFA] = 3000/1/1, mole ratio.

clearly indicate that the size, nature, and the ratio of [macro-CTA]/[Cat.] strongly influence the catalytic activity of the reaction and blocking efficiency for the resultant block copolymers.

Possible Reaction Mechanism. The possible explanation for influence on reactivity and blocking efficiency caused by changing the molecular weight and the amount of macro-CTAs is briefly described as follows. In the immortal copolymerization of epoxides/CO₂, the end-capped hydroxyl groups on the macro-CTA could be deprotonated to alkoxide ions as new initiating triggers (Scheme 1b). However, the number of active center could only be equal to the number of Zn complexes since the coupling reaction could only occur at the metal center in the reaction system. Consequently, two competitive reactions of the alkoxide ion would occur on the zinc center. That is, the active alkoxide ion would either incorporate in new CHO-alter-CO2 for chain growth or shuttle with dormant species via protonation to produce new dormant species in the system (Scheme 1b). Thus, when macro-CTAs were added into the reaction system, the rate related to the incorporation of CHO/CO₂ unit would be seriously suppressed by the surrounding dormant species via protonation reaction, resulting in low reactivity. For the inertness of the increasing molecular

weight of the macro-CTA, one possible factor is that due to the large hydrodynamic radius, the resulting macroinitiator has limited kinetic ability in the solution, which may slow down or prematurely stop chain growth, leading to retarded blocking efficiency.

Another possible reason for the influence on reactivity and blocking efficiency may be the compatibility between the macro-CTAs and PCHC. Taking PEG and PPG as examples, PPG and PEG have the similar chemical structure with only one carbon difference. However, when they worked as macro-CTAs, huge differences were detected during the coupling reaction of CHO/CO₂. Compared with PPG, we suspect that when the chain extension is initiated from hydrophilic PEG during the immortal polymerization (Scheme 1), the chain extension of the hydrophobic PCHC block may be disturbed by the complicated configurations and/or conformations of the active growth chain. Reversely, PPG has relative good compatibility with PCHC, and thereby the activity and blocking efficiency are better upon PPG utilization as macro-CTA in the CHO/CO₂ copolymerization. When PS-OH works as macro-CTA, the incompatibility between PS and PCHC arising from the distinct chemical structure may also lead to compromised activity and blocking efficiency. This explanation is reasonable

because similar experimental phenomenon and understanding have been reported in other chain transfer polymerizations. Structure 10 polymerization was detected even after 12 h (entry 12, Table 1). The possible factor is that the resulting polyamide has strong interactions to the metal center and/or to the initiating acetate ion which may prematurely stop chain growth. Nonetheless, we could not provide direct experimental evidence to support this assumption, and how the configurations and/or conformations of the active growth chain influence the reaction remains an open question.

Influence of Macro-CTAs on Reactivity and Blocking Efficiency during PO/CO₂ Copolymerization Using SalenCoX Complex. The immortal polymerizations in PO/CO₂ coupling reaction with different macro-CTAs under complex 2 (SalenCoTFA/PPN-TFA, TFA = trifluoroacetate, 1/1 mole ratio) were also performed (Table 2). The reaction condition was fixed at [PO]:[1] = 3000:1 and 2.0 MPa of CO₂. All the immortal polymerizations were monitored by *in situ* IR, and the detailed reaction conditions and results are illustrated in Table

Initially, PEG macro-CTA was selected as the model sample, and the effects on the activity and blocking efficiency were investigated by changing its molecular weight and varying the relative amounts of PEG to the catalyst. Each immortal polymerization was monitored by in situ IR detector, and the time-dependent signals at 1750 cm⁻¹ for the absorbance of PPC carbonyl group are provided in Figure 3A. Clearly, like the immortal copolymerization of CHO/CO₂ with 1, the reaction activity also decreases with the increase in the molecular weight and the amount of the macro-CTAs. For instance, when 1 equiv of PEG_{4K} was added, the TOF was 386 h⁻¹, while it decreased to 362 and 312 h⁻¹ upon addition of 5 and 10 equiv of PEG_{4K} (entries 1-3, Table 2). Once the molecular weight of PEG increased to 8.0 kg/mol, the catalytic activity toward PO sharply decreased from 290 h⁻¹ (1 equiv to 2) to 206 h⁻¹ after adding 5 times the amount of PEG_{8K} (entries 4 and 5, Table 2). Figure 3B displays the resultant GPC traces. Using PEG_{4K}, all polymers obtained from the reaction show bimodal GPC curves (a-d, Figure 3B). This situation is very similar to the immortal polymerization that during CHO/CO₂ coupling reaction under (BDI)ZnOAc complex. The shoulder with low retention volume (high molecular weight) could be assigned to PEG-b-PPC, and the shoulder with high retention volume (low molecular weight) was attributed to PPC homopolymers. When 5 equiv of PEG_{8K} was added in the reaction, unreacted PEG_{8K} was detected, and a GPC trace with triple shoulders clearly appeared (e, Figure 3B). Through chromatographic separation and followed by the NMR measurement, the composition of BCPs and the polymer degree of PPC blocks could be estimated by calculating the integral intensity of methylene (3.65 ppm) of PEG to the methine group (5.01 ppm) of PPC

After mathematical deconvolution of the GPC chromatograms, the area of the related block copolymers, PPC homopolymers, and unreacted macro-CTA could be well calculated. Following eqs 1 and 2, the blocking efficiency for each polymerization was obtained, and the results are provided in Table 2. When 5 and 10 equiv of amount of PEG $_{4K}$ were applied, the blocking efficiency increased to 60% and 78%, respectively, indicating that excess -OH groups from PEG ends could suppress the activity of the nucleophile anion X^- (trifluoroacetate) and hamper the formation of homo-PPC.

The blocking efficiency of using PEG_{4K} was 38% ($[PEG_{4K}]/[2]$ = 1/1, entry 1 in Table 2), while the measured value for PEG_{8K} decreased to 33% under the same conditions ($[PEG_{8K}]/[2]$ = 1/1, entry 4 in Table 2). When 5 equiv of PEG_{8K} was carried out for the chain transfer reaction, the blocking efficiency was decreased to 50%, which was much lower than the theoretical value 83% (entry 5, Table 2).

The decrease of catalytic activity with the increase of the molecular weight of macro-CTA and the ratio of macro-CTA]/[Cat.] was also observed for PPG and PS-OH (entries 6-12, Table 2). In contrast to PEG, however, the blocking efficiency of PPG is very close to the theoretical value. The infrared and nuclear magnetic resonance studies indicate that the variation of the molecular weight and the relative amounts of PPG macro-CTA have very mild impacts on the reactivity and the blocking efficiency in the immortal polymerizations (entries 6-8, Table 2). For PPGs, the value of the blocking efficiency is predictable, and the effect of variation of relative amounts is moderate (entries 6–8, Table 2). We postulate that PPG has good compatibility with the PPC block since they have the same unit, and both are hydrophobic blocks. Consequently, the macro-CTA with a dormant hydroxy group can rapidly shuttle with the active alkoxide species on the metal catalyst center, producing the predictable block copolymers.

Influence of Blocking Efficiency on Microphase Separation of the PS/PPC Block Copolymers. The selfassembling nature of block copolymer films has garnered a great deal of scientific interests due to its potential application in a variety of fields. 70 In the meanwhile, our interest in PPC/ PS block copolymers stems from the fact that we have demonstrated these are well-qualified polymers for the directed self-assembly strategy for the next-generation lithography. The advantage of PPC/PS block copolymer is derived from the fact that PPC and PS have equal surface energies; thus, simple thermal annealing could be performed to induce the nanostructures. Here, we aim to qualify how the blocking efficiency influences the assembly of the block copolymers. Two PPC-b-PS-b-PPC triblock copolymers with similar composition were collected by chain transfer polymerization of CO_2/PO using $\alpha_1\omega$ -dihydroxy end-capped polystyrene as CTA (entries 11 and 12, Table 2). The PPC-b-PS-b-PPC triblock copolymer with $M_n = 27.5$ kg/mol was prepared using 5 equiv of PS-OH_{12.5K} with blocking efficiency of 65% (abbreviated as BCP_{E65}), and the second one with similar molecular weight (28.1 kg/mol) was prepared by using 10 equiv of $PS\text{-}OH_{12.5K}$ with blocking efficiency of 76%(abbreviated as BCP_{E76}). The PPC volume ratios (f_{PPC}) of the two samples are around 50%, indicating the samples both have lamellae morphology. To study how PPC homopolymers influence the assembly, thin films of the two raw materials (before PPC homopolymers removed) were initially investigated. The thin films of samples ($\sim\!20$ nm thickness) were spun-coated on to PS-r-PMMA modified silicon wafers, and the wafers were annealed at 150 °C for 1 h. As shown in the SEM image in Figure 4A, the PPC-b-PS-b-PPC triblock copolymer with blocking efficiency of 65% show serious dewetting phenomenon, where perpendicular lamellae structure could not be observed because the PPC homopolymers were blended in the block copolymers. In contrast, defective lamellae structures with a large amount of cracks were located on the SEM image for the PPC-b-PS-b-PPC triblock copolymer with blocking efficiency of 76% as illustrated in Figure 4C.

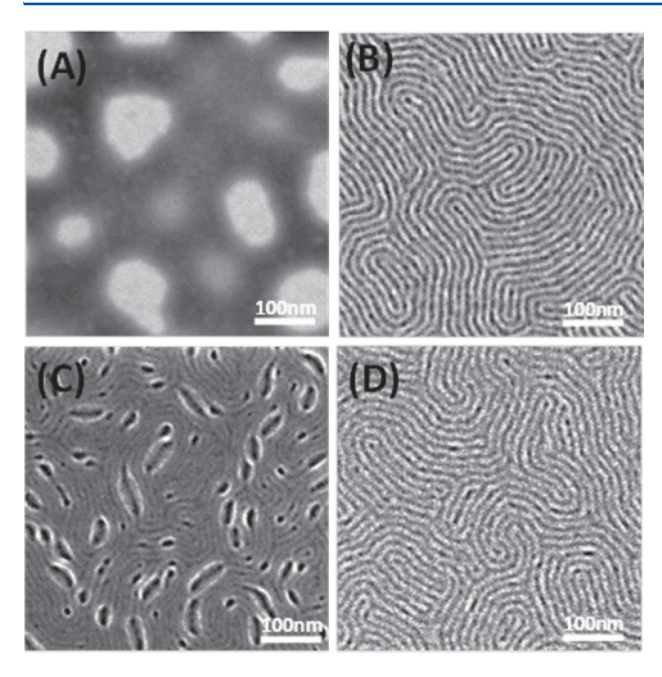


Figure 4. SEM images of PPC-b-PS-b-PPC thin films on silicon wafer coated with PS-r-PMMA brushes via thermal annealing. (A) Raw BCP_{E65} materials obtained by 5 equiv of PS-OH, (B) pure BCP_{E65} material after removing PPC contaminants, (C) raw BCP_{E76} material obtained using 10 equiv of PS-OH, and (D) pure BCP_{E76} material after removing PPC contaminants. Annealing conditions: 150 °C, 1 h; thickness of the thin film is \sim 20 nm.

Nevertheless, after removing the PPC contaminants, perfect lamellae structures with equal domain spacing (13.6 nm) were clearly detected on SEM images (Figure 4B,D) for the two samples, indicating the blocking efficiency has a serious impact on the nanoassembly.

CONCLUSION

In summary, several types of CO₂-based block copolymers were prepared by using various macro-CTAs including PPG, PEG, and PS empolying two classical catalyst systems. By analysis of the gel permeation chromatograms utilizing mathematical deconvolutions, the reaction activity and blocking efficiency for the resulting immortal polymerizations are systematically studied. On the basis of our study, it is clear that the size, nature, and the ratio of [macro-CTA]/[Cat.] strongly influence the catalytic activity and blocking efficiency of the reaction. Selfassembly of PS/PPC block copolymers clearly demonstrates that the blocking efficiency displays a serious impact on the nanoassembly. Although immortal copolymerization of epoxides/CO₂ with macro-CTA is a useful method for preparing CO₂-based block copolymer, the low blocking efficiency should be further considered in future studies, and a more effective process that gives higher quality CO2-based block copolymers is still desirable, thereby remaining a great challenge in polymer science.

AUTHOR INFORMATION

Corresponding Authors

*E-mail: gpwu@zju.edu.cn (G.-P.W.).

*E-mail: djdarens@chem.tamu.edu (D.J.D.).

ORCID (

Guang-Peng Wu: 0000-0001-8935-964X

Paul F. Nealey: 0000-0003-3889-142X

Donald J. Darensbourg: 0000-0001-9285-4895

Zhi-Kang Xu: 0000-0002-2261-7162

Notes

The authors declare no competing financial interest.

ACKNOWLEDGMENTS

Financial support is acknowledged to Qianjiang Talent-D Foundation (QJD1702025), National Natural Science Foundation of China (Grant 21674090), the National Science Foundation (CHE-1665258), and the Robert A. Welch Foundation (A-0923). G.-P.W. gratefully acknowledges the support of the "Hundred Talents Program" of Zhejiang University from China.

REFERENCES

- (1) Zhu, Y.; Romain, C.; Williams, C. K. Sustainable polymers from renewable resources. *Nature* **2016**, *540*, 354–362.
- (2) Darensbourg, D. J. Switchable catalytic processes involving the copolymerization of epoxides and carbon dioxide for the preparation of block polymers. *Inorg. Chem. Front.* **2017**, *4*, 412–419.
- (3) Luinstra, G. Poly(Propylene Carbonate), Old Copolymers of Propylene Oxide and Carbon Dioxide with New Interests: Catalysis and Material Properties. *Polym. Rev.* **2008**, *48*, 192–219.
- (4) Sugimoto, H.; Inoue, S. Copolymerization of carbon dioxide and epoxide. *J. Polym. Sci., Part A: Polym. Chem.* **2004**, *42*, 5561–5573.
- (5) Bottenbruch, L.; Anders, S. Engineering Thermoplastics: Polycarbonates, Polyacetals, Polyesters, Cellulose Esters; Hanser Verlag: 1996
- (6) Darensbourg, D. J. Making plastics from carbon dioxide: Salen metal complexes as catalysts for the production of polycarbonates from epoxides and CO₂. *Chem. Rev.* **2007**, *107*, 2388–2410.
- (7) Darensbourg, D. J.; Mackiewicz, R. M.; Phelps, A. L.; Billodeaux, D. R. Copolymerization of CO₂ and epoxides catalyzed by metal salen complexes. *Acc. Chem. Res.* **2004**, *37*, 836–844.
- (8) Kember, M. R.; Buchard, A.; Williams, C. K. Catalysts for CO₂/epoxide copolymerisation. *Chem. Commun.* **2011**, *47*, 141–163.
- (9) Chatterjee, C.; Chisholm, M. H. Influence of the Metal (Al, Cr, and Co) and the Substituents of the Porphyrin in Controlling the Reactions Involved in the Copolymerization of Propylene Oxide and Carbon Dioxide by Porphyrin Metal(III) Complexes. 2. Chromium Chemistry. *Inorg. Chem.* 2012, 51, 12041–12052.
- (10) Coates, G. W.; Moore, D. R. Discrete metal-based catalysts for the copolymerization of CO₂ and epoxides: discovery, reactivity, optimization, and mechanism. *Angew. Chem., Int. Ed.* **2004**, 43, 6618–6639.
- (11) Darensbourg, D. J.; Wilson, S. J. What's new with $\rm CO_2$? Recent advances in its copolymerization with oxiranes. *Green Chem.* **2012**, *14*, 2665–2671.
- (12) Lu, X.-B.; Ren, W.-M.; Wu, G.-P. CO₂ Copolymers from Epoxides: Catalyst Activity, Product Selectivity, and Stereochemistry Control. *Acc. Chem. Res.* **2012**, *45*, 1721–1735.
- (13) Lu, X.-B.; Darensbourg, D. J. Cobalt catalysts for the coupling of CO_2 and epoxides to provide polycarbonates and cyclic carbonates. Chem. Soc. Rev. 2012, 41 (4), 1462–1484.
- (14) Paul, S.; Zhu, Y.; Romain, C.; Brooks, R.; Saini, P. K.; Williams, C. K. Ring-opening copolymerization (ROCOP): synthesis and properties of polyesters and polycarbonates. *Chem. Commun.* **2015**, *51*, *6459–6479*.
- (15) Liu, Y.; Wang, M.; Ren, W.-M.; He, K.-K.; Xu, Y.-C.; Liu, J.; Lu, X.-B. Stereospecific CO₂ Copolymers from 3,5-Dioxaepoxides: Crystallization and Functionallization. *Macromolecules* **2014**, 47, 1269–1276.
- (16) Darensbourg, D. J.; Wilson, S. J. Synthesis of poly(indene carbonate) from indene oxide and carbon dioxide—a polycarbonate with a rigid backbone. *J. Am. Chem. Soc.* **2011**, *133*, 18610–18613.

(17) Hauenstein, O.; Reiter, M.; Agarwal, S.; Rieger, B.; Greiner, A. Bio-based polycarbonate from limonene oxide and CO₂ with high molecular weight, excellent thermal resistance, hardness and transparency. *Green Chem.* **2016**, *18*, 760–770.

- (18) Kindermann, N.; Cristòfol, À.; Kleij, A. W. Access to Biorenewable Polycarbonates with Unusual Glass-Transition Temperature (T_n) Modulation. ACS Catal. 2017, 7, 3860–3863.
- (19) Liu, Y.; Ren, W.-M.; Zhang, W.-P.; Zhao, R.-R.; Lu, X.-B. Crystalline CO₂-based polycarbonates prepared from racemic catalyst through intramolecularly interlocked assembly. *Nat. Commun.* **2015**, *6*, 8594.
- (20) Liu, Y.; Ren, W.-M.; He, K.-K.; Lu, X.-B. Crystalline-gradient polycarbonates prepared from enantioselective terpolymerization of meso-epoxides with CO₂. *Nat. Commun.* **2014**, *5*, 5687.
- (21) Wu, G.-P.; Xu, P.-X.; Lu, X.-B.; Zu, Y.-P.; Wei, S.-H.; Ren, W.-M.; Darensbourg, D. J. Crystalline CO_2 Copolymer from Epichlorohydrin via $\mathrm{Co}(\mathrm{III})$ -Complex-Mediated Stereospecific Polymerization. *Macromolecules* **2013**, *46*, 2128–2133.
- (22) Wu, G.-P.; Jiang, S.-D.; Lu, X.-B.; Ren, W.-M.; Yan, S.-K. Stereoregular poly(cyclohexene carbonate)s: Unique crystallization behavior. *Chin. J. Polym. Sci.* **2012**, *30*, 487–492.
- (23) Zhang, H.; Grinstaff, M. W. Synthesis of atactic and isotactic poly(1,2-glycerol carbonate)s: degradable polymers for biomedical and pharmaceutical applications. *J. Am. Chem. Soc.* **2013**, *135*, 6806–6809.
- (24) Honda, S.; Sugimoto, H. Carbon Dioxide-Derived Immortal Brush Macromolecules with Poly (propylene carbonate) Side Chains. *Macromolecules* **2016**, *49*, 6810–6816.
- (25) Hadjichristidis, N.; Pispas, S.; Floudas, G. Block Copolymers: Synthetic Strategies, Physical Properties, and Applications; John Wiley & Sons: 2003
- (26) Zhu, Y.; Romain, C.; Poirier, V.; Williams, C. K. Influences of a Dizinc Catalyst and Bifunctional Chain Transfer Agents on the Polymer Architecture in the Ring-Opening Polymerization of ε -Caprolactone. *Macromolecules* **2015**, 48, 2407–2416.
- (27) Kim, J. G.; Cowman, C. D.; LaPointe, A. M.; Wiesner, U.; Coates, G. W. Tailored Living Block Copolymerization: Multiblock Poly(cyclohexene carbonate)s with Sequence Control. *Macromolecules* **2011**, *44*, 1110–1113.
- (28) Darensbourg, D. J.; Ulusoy, M.; Karroonnirum, O.; Poland, R. R.; Reibenspies, J. H.; Cetinkaya, B. Highly Selective and Reactive (salan)CrCl Catalyst for the Copolymerization and Block Copolymerization of Epoxides with Carbon Dioxide. *Macromolecules* **2009**, 42, 6992–6998.
- (29) Nakano, K.; Hashimoto, S.; Nakamura, M.; Kamada, T.; Nozaki, K. Stereocomplex of Poly (propylene carbonate): Synthesis of Stereogradient Poly (propylene carbonate) by Regio- and Enantioselective Copolymerization of Propylene Oxide with Carbon Dioxide. *Angew. Chem., Int. Ed.* **2011**, 50, 4868–4871.
- (30) Jeske, R. C.; Rowley, J. M.; Coates, G. W. Pre-rate-determining selectivity in the terpolymerization of epoxides, cyclic anhydrides, and CO₂: A one-step route to diblock copolymers. *Angew. Chem., Int. Ed.* **2008**, 47, 6041–6044.
- (31) Huijser, S.; HosseiniNejad, E.; Sablong, R.; de Jong, C.; Koning, C. E.; Duchateau, R. Ring-Opening Co- and Terpolymerization of an Alicyclic Oxirane with Carboxylic Acid Anhydrides and CO₂ in the Presence of Chromium Porphyrinato and Salen Catalysts. *Macromolecules* **2011**, *44*, 1132–1139.
- (32) Darensbourg, D. J.; Poland, R. R.; Escobedo, C. Kinetic Studies of the Alternating Copolymerization of Cyclic Acid Anhydrides and Epoxides, and the Terpolymerization of Cyclic Acid Anhydrides, Epoxides, and CO₂ Catalyzed by (salen) CrIIICl. *Macromolecules* **2012**, 45, 2242–2248.
- (33) Liu, Y.; Deng, K.; Wang, S.; Xiao, M.; Han, D.; Meng, Y. A novel biodegradable polymeric surfactant synthesized from carbon dioxide, maleic anhydride and propylene epoxide. *Polym. Chem.* **2015**, *6*, 2076–2083.
- (34) Liu, Y.; Xiao, M.; Wang, S.; Xia, L.; Hang, D.; Cui, G.; Meng, Y. Mechanism studies of terpolymerization of phthalic anhydride,

propylene epoxide, and carbon dioxide catalyzed by ZnGA. RSC Adv. 2014, 4, 9503–9508.

- (35) Van Zee, N. J.; Sanford, M. J.; Coates, G. W. Electronic Effects of Aluminum Complexes in the Copolymerization of Propylene Oxide with Tricyclic Anhydrides: Access to Well-Defined, Functionalizable Aliphatic Polyesters. *J. Am. Chem. Soc.* **2016**, *138*, 2755–2761.
- (36) Duan, Z.; Wang, X.; Gao, Q.; Zhang, L.; Liu, B.; Kim, I. Highly Active Bifunctional Cobalt-Salen Complexes for the Synthesis of Poly(ester-block-carbonate) Copolymer via Terpolymerization of Carbon Dioxide, Propylene Oxide, and Norbornene Anhydride Isomer: Roles of Anhydride Conformation Consideration. *J. Polym. Sci., Part A: Polym. Chem.* 2014, 52, 789–795.
- (37) Kernbichl, S.; Reiter, M.; Adams, F.; Vagin, S.; Rieger, B. CO_2 -Controlled One-Pot Synthesis of AB, ABA Block, and Statistical Terpolymers from β -Butyrolactone, Epoxides, and CO_2 . *J. Am. Chem. Soc.* **2017**, *139*, *6787*–*6790*.
- (38) Kember, M. R.; Williams, C. K. Efficient magnesium catalysts for the copolymerization of epoxides and CO₂; using water to synthesize polycarbonate polyols. *J. Am. Chem. Soc.* **2012**, *134*, 15676–15679.
- (39) Jutz, F.; Buchard, A.; Kember, M. R.; Fredriksen, S. B.; Williams, C. K. Mechanistic investigation and reaction kinetics of the low-pressure copolymerization of cyclohexene oxide and carbon dioxide catalyzed by a dizinc complex. J. Am. Chem. Soc. 2011, 133, 17395—17405
- (40) Inoue, S. Immortal polymerization: The outset, development, and application. *J. Polym. Sci., Part A: Polym. Chem.* **2000**, 38, 2861–2871.
- (41) Aida, T.; Inoue, S. Metalloporphyrins as initiators for living and immortal polymerizations. *Acc. Chem. Res.* **1996**, 29, 39–48.
- (42) Cyriac, A.; Lee, S. H.; Varghese, J. K.; Park, E. S.; Park, J. H.; Lee, B. Y. Immortal CO₂/Propylene Oxide Copolymerization: Precise Control of Molecular Weight and Architecture of Various Block Copolymers. *Macromolecules* **2010**, *43*, 7398–7401.
- (43) Kember, M. R.; Copley, J.; Buchard, A.; Williams, C. K. Triblock copolymers from lactide and telechelic poly(cyclohexene carbonate). *Polym. Chem.* **2012**, *3*, 1196–1201.
- (44) Wu, G.-P.; Darensbourg, D. J. Mechanistic Insights into Water-Mediated Tandem Catalysis of Metal-Coordination CO₂/Epoxide Copolymerization and Organocatalytic Ring-Opening Polymerization: One-Pot, Two Steps, and Three Catalysis Cycles for Triblock Copolymers Synthesis. *Macromolecules* **2016**, *49*, 807–814.
- (45) Wu, G.-P.; Darensbourg, D. J.; Lu, X.-B. Tandem Metal-Coordination Copolymerization and Organocatalytic Ring-Opening Polymerization via Water To Synthesize Diblock Copolymers of Styrene Oxide/CO₂ and Lactide. *J. Am. Chem. Soc.* **2012**, *134*, 17739–17745.
- (46) Darensbourg, D. J.; Wu, G.-P. A One-Pot Synthesis of a Triblock Copolymer from Propylene Oxide/Carbon Dioxide and Lactide: Intermediacy of Polyol Initiators. *Angew. Chem., Int. Ed.* **2013**, 52, 10602–10606.
- (47) Reiter, M.; Kronast, A.; Kissling, S.; Rieger, B. In Situ Generated ABA Block Copolymers from CO₂, Cyclohexene Oxide, and Poly(dimethylsiloxane)s. ACS Macro Lett. **2016**, *5*, 419–423.
- (48) Zhang, D.; Zhang, H.; Hadjichristidis, N.; Gnanou, Y.; Feng, X. Lithium-Assisted Copolymerization of $\rm CO_2/Cyclohexene$ Oxide: A Novel and Straightforward Route to Polycarbonates and Related Block Copolymers. *Macromolecules* **2016**, *49*, 2484–2492.
- (49) Hilf, J.; Schulze, P.; Frey, H. CO₂-Based Non-ionic Surfactants: Solvent-Free Synthesis of Poly(ethylene glycol)-block-Poly(propylene carbonate) Block Copolymers. *Macromol. Chem. Phys.* **2013**, 214, 2848–2855.
- (50) Wang, Y.; Fan, J.; Darensbourg, D. J. Construction of Versatile and Functional Nanostructures Derived from CO₂-based Polycarbonates. *Angew. Chem., Int. Ed.* **2015**, *54*, 10206–10210.
- (51) Cowman, C. D.; Padgett, E.; Tan, K. W.; Hovden, R.; Gu, Y.; Andrejevic, N.; Muller, D.; Coates, G. W.; Wiesner, U. Multicomponent Nanomaterials with Complex Networked Architectures from Orthogonal Degradation and Binary Metal Backfilling in ABC Triblock Terpolymers. J. Am. Chem. Soc. 2015, 137, 6026–6033.

(52) Yang, G.-W.; Wu, G.-P.; Chen, X.; Xiong, S.; Arges, C. G.; Ji, S.; Nealey, P. F.; Lu, X.-B.; Darensbourg, D. J.; Xu, Z.-K. Directed Self-Assembly of Polystyrene-b-poly(propylene carbonate) on Chemical Patterns via Thermal Annealing for Next Generation Lithography. *Nano Lett.* 2017, 17, 1233–1239.

- (53) Childers, M. I.; Vitek, A. K.; Morris, L. S.; Widger, P. C. B.; Ahmed, S. M.; Zimmerman, P. M.; Coates, G. W. Isospecific, Chain Shuttling Polymerization of Propylene Oxide Using a Bimetallic Chromium Catalyst: A New Route to Semicrystalline Polyols. *J. Am. Chem. Soc.* 2017, 139, 11048–11054.
- (54) Valente, A.; Mortreux, A.; Visseaux, M.; Zinck, P. Coordinative chain transfer polymerization. *Chem. Rev.* **2013**, *113*, 3836–3857.
- (55) Stoykovich, M. P.; Muller, M.; Kim, S. O.; Solak, H. H.; Edwards, E. W.; de Pablo, J. J.; Nealey, P. F. Directed assembly of block copolymer blends into nonregular device-oriented structures. *Science* **2005**, 308, 1442–1446.
- (56) Cheng, M.; Moore, D. R.; Reczek, J. J.; Chamberlain, B. M.; Lobkovsky, E. B.; Coates, G. W. Single-site β -diiminate zinc catalysts for the alternating copolymerization of CO_2 and epoxides: Catalyst synthesis and unprecedented polymerization activity. *J. Am. Chem. Soc.* **2001**, *123*, 8738–8749.
- (57) Berkessel, A.; Brandenburg, M. Catalytic asymmetric addition of carbon dioxide to propylene oxide with unprecedented enantioselectivity. *Org. Lett.* **2006**, *8*, 4401–4404.
- (58) Bartels, J. W.; Cauet, S. I.; Billings, P. L.; Lin, L. Y.; Zhu, J.; Fidge, C.; Pochan, D. J.; Wooley, K. L. Evaluation of Isoprene Chain Extension from PEO Macromolecular Chain Transfer Agents for the Preparation of Dual, Invertible Block Copolymer Nanoassemblies. *Macromolecules* 2010, 43, 7128–7138.
- (59) Gao, H.; Tsarevsky, N. V.; Matyjaszewski, K. Synthesis of Degradable Miktoarm Star Copolymers via Atom Transfer Radical Polymerization. *Macromolecules* **2005**, *38*, 5995–6004.
- (60) Jennings, J.; Beija, M.; Kennon, J. T.; Willcock, H.; O'Reilly, R. K.; Rimmer, S.; Howdle, S. M. Advantages of Block Copolymer Synthesis by RAFT-Controlled Dispersion Polymerization in Supercritical Carbon Dioxide. *Macromolecules* **2013**, *46*, 6843–6851.
- (61) Cheng, M.; Lobkovsky, E. B.; Coates, G. W. Catalytic Reactions Involving C1Feedstocks: New High-Activity Zn(II)-Based Catalysts for the Alternating Copolymerization of Carbon Dioxide and Epoxides. *J. Am. Chem. Soc.* **1998**, *120*, 11018–11019.
- (62) Allen, S. D.; Moore, D. R.; Lobkovsky, E. B.; Coates, G. W. High-activity, single-site catalysts for the alternating copolymerization of CO_2 and propylene oxide. *J. Am. Chem. Soc.* **2002**, *124*, 14284–14285.
- (63) Moore, D. R.; Cheng, M.; Lobkovsky, E. B.; Coates, G. W. Mechanism of the alternating copolymerization of epoxides and CO_2 using β -diiminate zinc catalysts: Evidence for a bimetallic epoxide enchainment. *J. Am. Chem. Soc.* **2003**, 125, 11911–11924.
- (64) Cohen, C. T.; Chu, T.; Coates, G. W. Cobalt catalysts for the alternating copolymerization of propylene oxide and carbon dioxide: combining high activity and selectivity. *J. Am. Chem. Soc.* **2005**, *127*, 10869—10878
- (65) Lu, X.-B.; Shi, L.; Wang, Y.-M.; Zhang, R.; Zhang, Y.-J.; Peng, X.-J.; Zhang, Z.-C.; Li, B. Design of highly active binary catalyst systems for CO₂/epoxide copolymerization: polymer selectivity, enantioselectivity, and stereochemistry control. *J. Am. Chem. Soc.* **2006**, *128*, 1664–1674.
- (66) Wang, Y.-M.; Song, X.-Y.; Shao, S.-H.; Xu, P.-X.; Ren, W.-M.; Lu, X.-B. Functionalization of carbon nanotubes by surface-initiated immortal alternating polymerization of CO_2 and epoxides. *Polym. Chem.* **2013**, *4*, 629–636.
- (67) Shi, L.; Lu, X.-B.; Zhang, R.; Peng, X.-J.; Zhang, C.-Q.; Li, J.-F.; Peng, X.-M. Asymmetric alternating copolymerization and terpolymerization of epoxides with carbon dioxide at mild conditions. *Macromolecules* **2006**, *39*, 5679–5685.
- (68) Ren, W.-M.; Liu, Z.-W.; Wen, Y.-Q.; Zhang, R.; Lu, X.-B. Mechanistic aspects of the copolymerization of CO₂ with epoxides using a thermally stable single-site cobalt (III) catalyst. *J. Am. Chem. Soc.* **2009**, *131*, 11509–11518.

(69) The GPC molecular weight is lower than the theoretical value and is attributed to the polystyrene calibration.

(70) Kim, H.-C.; Park, S.-M.; Hinsberg, W. D. Block Copolymer Based Nanostructures: Materials, Processes, and Applications to Electronics. *Chem. Rev.* **2010**, *110*, 146–177.